Journal of Applied Mechanics and Technical Physics, Vol. 37, No. 5, 1996

HEAT PROPAGATION FROM A LINE SOURCE IN A PLANE TURBULENT WAKE

V. I. Bukreev,[1] A. G. Demenkov,[2]
V. A. Kostomakha,[1] and G. G. Chernykh[2]

UDC 532.517.4

The transport of a passive admixture (heat from a line source) in a plane turbulent wake behind a cylinder with an elliptical cross section is experimentally investigated for the case where the source is positioned outside the wake symmetry plane. This flow is numerically simulated using a number of semi-empirical turbulence models. The specified, initially asymmetric temperature distribution in the wake is shown to tend to the same type of symmetry as the distributions of the averaged velocity-field characteristics, but the "memory" about the location of an admixture source is erased extremely slowly. Satisfactory agreement between the computed and experimental results is obtained.

1. The transport of various admixtures by turbulent flows is a common phenomenon both in nature and technology. This explains the keen interest in theoretical description of the transport processes and their experimental investigation. The following most important problems are usually solved: What are the space-time distributions of the admixture concentration, how does the concentration decrease with distance from the source, what part of the region is occupied by the admixture, are the admixture-concentration distributions transformed to some asymptotic form, etc?

For the below-considered case of a continuous line source placed in various turbulent flows, the following information is available in the literature. In a field of homogeneous isotropic turbulence, the distribution of the averaged admixture concentration is described by the Gaussian curve [1, 2]. The features of the behavior were established which are typical of the variance of transverse displacements of a labeled "liquid" particle that characterizes the admixture cloud dimensions, and also of the maximum admixture concentration at small or large distances (or times) from the source. Note that the variance mentioned was calculated using the above distributions. The suggested semi-empirical turbulence models ensure a satisfactory description of such flows [3].

The presence of a constant shift of the mean velocity in a field of homogeneous turbulence [4–6] leads to asymmetric concentration distributions and, as in isotropic turbulence, to a faster growth of the dimensions of an admixture cloud with almost the same decrease in maximum concentration. For shearless inhomogeneous turbulence the temperature profiles behind a line heat source are also essentially asymmetric [7].

The authors of [8, 9] have studied the heat diffusion from a line source placed into a turbulent boundary layer on a flat plate at different distances from the wall. It was found in the experiments that the transverse profiles of the mean temperature tend to an asymptotic distribution that is independent of the source position.

The behavior of an admixture distributed inhomogeneously in the initial cross section of a turbulent wake or a jet is poorly known. The only experimental data on the heat diffusion from a line source in a plane turbulent jet presented in [1] are obtained for moderate distances from the source and give no idea of the possibility of attaining the asymptotic form of the concentration distributions and of its character. The decay laws of the admixture concentration derived in [2] are valid only for self-similar flow regimes in a jet or a wake at great distances from the source.

[1]Lavrent'ev Institute of Hydrodynamics, Siberian Division, Russian Academy of Sciences, Novosibirsk 630090. [2]Institute of Computational Technologies, Siberian Division, Russian Academy of Sciences, Novosibirsk 630090. Translated from Prikladnaya Mekhanika i Tekhnicheskaya Fizika, Vol. 37, No. 5, pp. 115–126, September–October, 1996. Original article submitted July 15, 1995.

 0021-8944/96/3705-0710 $15.00

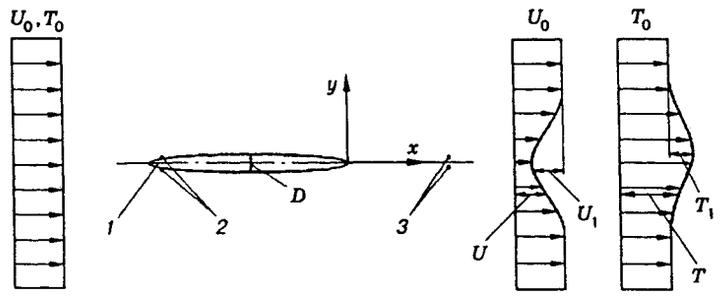

Fig. 1

The goal of the present work is to obtain new experimental information on the propagation of a passive admixture in a plane wake behind a cylinder and to demonstrate the possibilities of mathematical simulation of transport processes in such a flow.

2. The flow is described by the following system of averaged equations of motion and heat transfer in a thin-shear-layer approximation:

$$U\frac{\partial U}{\partial x} + V\frac{\partial U}{\partial y} = -\frac{\partial}{\partial y}\langle u'v'\rangle; \tag{2.1}$$

$$\frac{\partial U}{\partial x} + \frac{\partial V}{\partial y} = 0; \tag{2.2}$$

$$U\frac{\partial T}{\partial x} + V\frac{\partial T}{\partial y} = -\frac{\partial}{\partial y}\langle v'T'\rangle. \tag{2.3}$$

Here U and V are the horizontal and vertical components of the averaged velocity; u', v', and T' are the fluctuation components of velocity and temperature; T is the averaged fluid temperature in the wake; $\langle u'v'\rangle$ is the tangential Reynolds stress; and $\langle v'T'\rangle$ is the vertical component of the turbulent-heat-flux vector; the angle brackets denote averaging. Assuming that the terms with molecular viscosity and diffusion are small, we ignore them in the equations.

The flow diagram and the coordinate system used are presented in Fig. 1.

The system (2.1)–(2.3) is not closed. To close Eq. (2.1), we use the relation

$$-\langle u'v'\rangle = \nu_t\frac{\partial U}{\partial y}.$$

Two variants of representation of the turbulent viscosity ν_t were considered. In the first one, it was assumed [10] that $\nu_t = c_\mu e^2/\varepsilon$.

To determine the turbulence energy e, the following equation was used:

$$U\frac{\partial e}{\partial x} + V\frac{\partial e}{\partial y} = \frac{\partial}{\partial y}\nu_t\frac{\partial e}{\partial y} + P - \varepsilon. \tag{2.4}$$

The dissipation rate ε was found using Kolmogorov's relation

$$\varepsilon = \alpha e^{3/2}/L, \tag{2.5}$$

where L is the reference scale of the turbulent flow defined by

$$e(x, L) = e(x, 0)/2.$$

The quantity P in Eq. (2.4) is the generation of turbulence energy due to the averaged motion:

$$P = \nu_t\left(\frac{\partial U}{\partial y}\right)^2.$$

In the second variant, the turbulent viscosity ν_t was defined as [10]

$$\nu_t = \frac{2}{3}\Phi\left(1 - \frac{P}{\varepsilon}\Phi\right)\frac{e^2}{\varepsilon}, \quad \Phi = \frac{1 - C_2}{C_1 - 1 + \frac{P}{\varepsilon}}. \tag{2.6}$$

The dissipation rate ε was found by solution of the differential transport equation

$$U\frac{\partial \varepsilon}{\partial x} + V\frac{\partial \varepsilon}{\partial y} = \frac{\partial}{\partial y}\frac{\nu_t}{\sigma_\varepsilon}\frac{\partial \varepsilon}{\partial y} + \frac{\varepsilon}{e}(C_{\varepsilon 1}P - C_{\varepsilon 2}\varepsilon). \tag{2.7}$$

The quantities C_μ, α, C_1, C_2, σ_ε, $C_{\varepsilon 1}$, and $C_{\varepsilon 2}$ are empirical constants.

It is well known that a mathematical model of turbulent jet flows that includes Eqs. (2.4) and (2.7), and expression (2.6) for turbulent viscosity is fairly universal [10–13]. However, this model leads to difficulties in specifying the initial conditions for ε because of the lack of necessary experimental data. In this connection, as in [11, 12], the mathematical model including Eq. (2.4) and relation (2.5) was employed not only to calculate, but also to determine the initial distribution of ε in more complex models.

As for the closure of Eq. (2.3), two approaches were also considered. In the first one, it was assumed that [13]

$$-\langle v'T'\rangle = \nu_{tT}\frac{\partial T}{\partial y}, \quad \nu_{tT} = \frac{2}{3}\Phi_T\left(1 - \frac{P}{\varepsilon}\Phi\right)\frac{e^2}{\varepsilon}, \tag{2.8}$$

$$\Phi_T = \left[C_{1T} + \frac{1}{2}\left(\frac{P}{\varepsilon} - 1\right) + \frac{1}{2}\frac{e}{\varepsilon}\frac{\varepsilon_T}{\langle T'^2\rangle}\left(\frac{P_T}{\varepsilon_T} - 1\right)\right]^{-1}, \quad P_T = -2\langle v'T'\rangle\frac{\partial T}{\partial y}.$$

In addition, the equation for the transformation of the temperature fluctuation variance $\langle T'^2\rangle$ was used:

$$U\frac{\partial \langle T'^2\rangle}{\partial x} + V\frac{\partial \langle T'^2\rangle}{\partial y} = \frac{\partial}{\partial y}\nu_{tT}\frac{\partial \langle T'^2\rangle}{\partial y} - 2\langle v'T'\rangle\frac{\partial T}{\partial y} - \varepsilon_T. \tag{2.9}$$

The algebraic approximation from [13] was used for the smoothing rate ε_T of temperature inhomogeneities:

$$\varepsilon_T = C_T\frac{\varepsilon\langle T'^2\rangle}{e}. \tag{2.10}$$

The second approach implied the use of the differential equation from [10] to find $\langle v'T'\rangle$:

$$U\frac{\partial \langle v'T'\rangle}{\partial x} + V\frac{\partial \langle v'T'\rangle}{\partial y} = \frac{\partial}{\partial y}\nu'_{tT}\frac{\partial \langle v'T'\rangle}{\partial y} - \langle v'^2\rangle\frac{\partial T}{\partial y} - C_{1T}\frac{\varepsilon}{e}\langle v'T'\rangle - (1 - C_{2T})\langle v'T'\rangle\frac{\partial V}{\partial y}. \tag{2.11}$$

The turbulent diffusion ν'_{tT} was determined as

$$\nu'_{tT} = C_{\theta 1}\frac{2}{3}\left(1 - \frac{P}{\varepsilon}\Phi\right)\frac{e^2}{\varepsilon} = C_{\theta 1}\frac{\langle v'^2\rangle e}{\varepsilon}. \tag{2.12}$$

In Eq. (2.9), ν_{tT} was replaced by $\nu''_{tT} = C_{\theta 2}\langle v'^2\rangle e/\varepsilon$. The quantities C_T, C_{1T}, C_{2T}, $C_{\theta 1}$, and $C_{\theta 2}$ in relations (2.8), (2.10), and (2.12) are empirical constants. In this paper we use two different methods of determining $\langle v'T'\rangle$ [algebraic approximation (2.8) and differential equation (2.11)], because comparison of numerical data of different models is another criterion of reliability of results of mathematical simulation.

Taking into account the above considerations, we formulate three mathematical models, all including Eqs. (2.1)–(2.3) and (2.9). Model No. 1 is supplemented by Eqs. (2.4) and (2.11) and also by relations (2.5) and (2.10); model No. 2 employs Eqs. (2.4), (2.7), and (2.11), and also relations (2.6) and (2.10); model No. 3 also employs Eqs. (2.4) and (2.7) and relations (2.6), (2.8), and (2.10).

3. The variable x plays the role of time in the problem under consideration. At $x = x_0$, the initial distributions of U, T, e, ε, $\langle T'^2\rangle$, and $\langle v'T'\rangle$ are specified in accordance with experimental data. The zero values of the averaged velocity $U_1 = U_0 - U$ and temperature $T_1 = T - T_0$ defects, and also of the quantities e, ε, $\langle T'^2\rangle$, and $\langle v'T'\rangle$, are used as the boundary conditions for $|y| \to \infty$. Here U_0 and T_0 are the free-stream

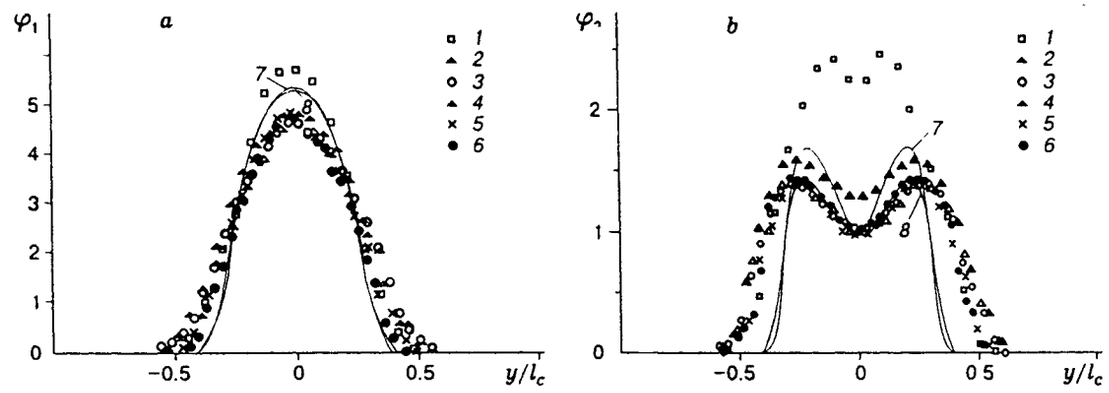

Fig. 2

velocity and temperature. The problem is formulated for the most complete model No. 2. For model Nos. 1 and 3, the problem is formulated in a similar way.

The variables of the problem are made dimensionless using the reference scales for velocity U_0, temperature T_*, and length L_*.

4. To construct a finite-difference algorithm, we introduce a stream function ψ ($U = \partial\psi/\partial y$ and $V = -\partial\psi/\partial x$). The desired functions (we use model No. 2 for illustration) are U, ψ, T, e, ε, $\langle v'T'\rangle$, and $\langle T'^2\rangle$. The details of construction of a finite-difference analog of the problem using movable grids and an example of its realization for isothermic flows are given in [14]. Introduction of additional equations into the mathematical model for nonisothermic flows produces a minor complication in the algorithm. As the results of our numerical experiments show, stationary uniform grids and central-difference approximations of convective terms can be used in the problems considered.

The algorithm was thoroughly tested in [14]. The numerical results below demonstrate the application of model Nos. 2 and 3 to numerical investigation of the flow in a plane wake behind a heated cylinder under laboratory experimental conditions [15]. The initial distributions were specified for $x/D = 625$. The cylinder diameter D was chosen as L_*, and the temperature T_* was assumed to be equal to T_0. The following set of empirical constants was used in computations by model No. 2: $C_\mu = 0.09$, $C_1 = 2.2$, $C_2 = 0.55$, $C_{\varepsilon 1} = 1.44$, $C_{\varepsilon 2} = 1.92$, $C_T = 1.7$, $C_{1T} = 3.2$, $C_{2T} = 0.5$, $C_{\theta 1} = 0.22$, and $C_{\theta 2} = 0.13$. In model No. 3, the empirical constant C_T was assumed to be equal to 2.3. All the empirical constants, except for $C_{\theta 1}$, $C_{\theta 2}$, and C_T, are commonly used. Computations were carried out on a uniform difference grid. The discretization parameters δx and δy with respect to the variables x and y were chosen equal to $0.5D$ and $0.2D$, respectively. A fourfold reduction of δx with a simultaneous twofold reduction of δy caused deviations as small as 1% (in a norm that is a grid analog of the norm of the space of continuous functions). Computations were performed within the domain $x/D \geqslant 625$ and $0 \leqslant y/D \leqslant 40$.

The numerical and experimental results are compared in Fig. 2. Figure 2a shows the self-similar profiles of averaged temperature $\varphi_1(y/l_c) = T_1/T_c$ and Fig. 2b presents the self-similar distributions of temperature-fluctuation intensities $\varphi_2(y/l_c) = \langle T'^2\rangle^{1/2}/T_c$, where $l_c = (x - x_v)^{1/2}D^{1/2}$, $T_c = (8.5\,^\circ\mathrm{C})D^{1/2}(x - x_v)^{-1/2}$, and x_v is the virtual origin of the coordinates. The experimental data obtained for different values of x/D are shown by points 1–6, and curves 7 and 8 indicate computations by model Nos. 2 and 3, respectively. The agreement between the computed and experimental data is satisfactory.

5. Experiments were performed in a wind tunnel with a closed test section with length 4 m and reference transverse size 0.4 m. The test section was slightly expanded downstream so as to compensate for the momentum loss because of the growth of the boundary layers. For a mean-flow velocity of 15 m/sec in the core, the longitudinal pressure gradient was equal to zero.

An elliptic cylinder 1 (see Fig. 1) with ratio of axes equal to six was mounted at 30 cm from the beginning of the test section and was oriented at the zero angle of attack with respect to the free stream.

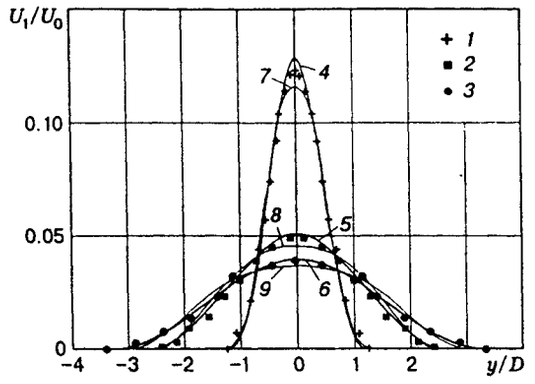

Fig. 3

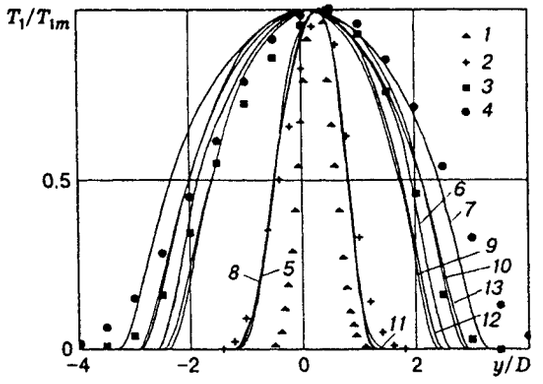

Fig. 4

Turbulizing wires 2 of 1 mm diameter were fixed to its surface 3 mm from the leading edge. The elliptic cylinder was the same as in [16]. The experiments were performed at Reynolds number $\mathrm{Re} = U_0 D/\nu = 1.1 \cdot 10^4$. Here $D = 10.4$ mm is the minor axis of the ellipse (the cross section of the cylinder), ν is the kinematic viscosity, and $U_0 = 15.4$ m/sec. The line heat sources were thin 0.3-mm-diameter nichrome wires 3 heated by an electric current, positioned in the cross section $x = 3D$ at $y = \pm 0.19D$, and directed along the z axis. A constant heating regime for the wires was maintained by controlling the electric current. Either the upper ($y = 0.19D$) or the lower ($y = -0.19D$) wire were heated in the experiments.

The mean velocity was measured using total- and static-pressure tubes fabricated from medical needles 1.1 mm in diameter. The mean temperature was measured by an ST3-18 bead temperature-sensitive resistor whose diameter was 0.5 mm. A DISA55D05 hot-wire anemometer allowed one to duplicate the measurements of U and T and to obtain information on the values of $\langle u'^2 \rangle$ and $\langle T'^2 \rangle$. The method of three overheatings was used [17]. The hot wire was 5 μm in diameter and 1.25 mm long. The temperature-sensitive resistor and the hot-wire anemometer were preliminarily calibrated to determine their sensitivity to velocity and temperature.

6. The profiles of U_1 and $\langle u'^2 \rangle$ were measured in some cross sections of the wake behind the cylinder without heating wires. A comparison of the obtained data with those measured previously in [16] shows their good (within the experimental error) coincidence. This, in turn, allowed us to use the results of the experiments in [16] as reference data to assess the influence of heating wires on wake dynamics.

Figure 3 shows the transverse distributions of U_1 measured experimentally in the presence of heating wires. Points 1–3 correspond to distances from the cylinder $x/D = 18$, 120, and 200, respectively. Since the cylinder was specially mounted at zero angle of attack, the $U_1(y)$ profiles are symmetric about the plane $y = 0$.

For small x/D, the presence of heating wires stimulated the growth in the velocity defect near the symmetry plane of the wake, unlike the data of [16]. This discrepancy is explained by the fact that every wire generates its own wakes that interact with each other and introduce additional disturbances into the cylinder wake. However, the contribution of these disturbances decreases with an increase in x/D because of decay, and, beginning with $x/D \geqslant 36$, the distributions of $U_1(y)$ are practically the same as those measured in [16]. Thus, the drag coefficient per unit length of the cylinder was independent of the presence of heated wires in the wake and was equal to 0.26, as in [16].

Curves 4–6 in Fig. 3 are the results of calculations by model No. 1 for cross sections $x/D = 18$, 120, and 200, respectively; curves 7–9 are the results of similar numerical calculations by model No. 2. Model No. 3 yields the same distributions as model No. 2. The empirical constants for model Nos. 1–3 were the same as in the previous description of the wake behind a fully heated cylinder (see Section 4). The value of $\alpha = 0.82$ was chosen from the conditions of agreement with the experimental data of the present work. The grid parameters were $\delta x = 0.1D$ and $\delta y = 0.04D$. A simultaneous reduction of δy by a factor of two and of δx by a factor of four gives computation results with a difference not greater than 0.5% in the uniform norm. The initial data were given for $x/D = 9$.

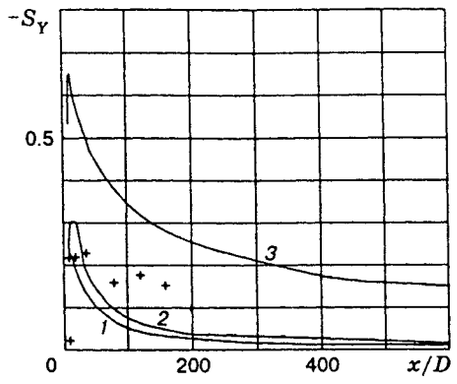

Fig. 5

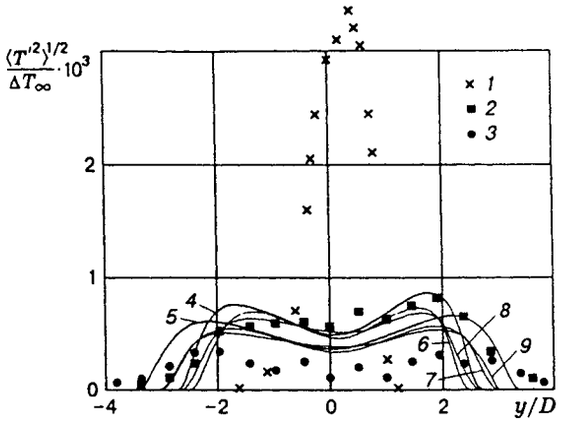

Fig. 6

To verify that the heat introduced into the wake can be regarded as a passive admixture and the buoyancy force effect can be ignored, we measured the distributions of the mean velocity and of the turbulence intensity of the longitudinal velocity component in a nonisothermic wake. These distributions in a heated wake were found to remain symmetric about the plane $y = 0$ and practically coincided with the corresponding turbulence characteristics measured in the isothermic wake.

The transverse profiles of excess temperatures T_1^+ and T_1^- that correspond to heating of either the upper or the lower wire were experimentally measured. The T_1^+ distributions were found to be mirror-symmetric (about the plane $y = 0$) to the T_1^- profiles within the experimental error: $[T_1^+(y) = T_1^-(-y)]$. This result is additional evidence that the buoyancy forces have no effect on the heated-wake evolution. Below we give only the characteristics of the behavior of a passive admixture, which were measured with heating of the upper wire (the superscript plus is omitted everywhere below).

Figure 4 shows the measured profiles of the dimensionless temperature T_1/T_{1m}, where T_{1m} is the maximum value of T_1 in the given cross section, and points 1–4 correspond to $x/D = 5$, 18, 120, and 200. One can see that the T_1 distributions at moderate distances downstream from the heat source are symmetric about a straight line that is parallel to the plane $y = 0$ and passes through the heated wire. However, the heat propagation over the wake cross section becomes noticeably asymmetric with distance from the source. The heated fluid elements are transported predominantly to the central part of the wake, i.e., to the region of lower velocities. It should be noted that a qualitatively similar picture of heat diffusion from a line source was observed in [1] in a plane jet in which a passive admixture added outside the jet symmetry plane was also transferred mainly to its central region, in which, unlike a plane wake, the velocities are maximal.

Curves 5–7 illustrate the data computed using model No. 1 for $x/D = 18$, 120, and 200; curves 8–10 and 11–13 are the results obtained by model Nos. 2 and 3, respectively.

The data in Fig. 4 show that the $T_1(y)$ profiles remain asymmetric up to the largest distances x/D examined in the experiments, and it is not clear whether they preserve their asymmetry far downstream. If the first possibility is realizable, this means that the temperature field characteristics "remember" the location of an admixture source. Otherwise, one must conclude that the "memory" about the place of admixture introduction into the wake behind the cylinder is erased.

To obtain additional information on the question of interest, we calculated the skewness s_Y of the probability-distribution density $P(Y)$ for the Lagrangian coordinate Y of a "labeled" liquid particle that is numerically equal to the distance of this particle from the source plane at the instant $\tau = x'/U$, where $x' = x - 3D$. The quantity s_Y is very sensitive to small variations of the function $P(Y)$, which is determined, in a fixed cross section of the wake, by the averaged concentration of the passive admixture (in the given case,

of excess temperature) [1, 2]:

$$P(Y) = \frac{T_1(y)}{\int_{-\infty}^{\infty} T_1(y)dy}.$$

The value of s_Y was calculated by the formula

$$s_Y = (1/\sigma_Y^3)\int_{-\infty}^{\infty}(Y-\overline{Y})^3 P(Y)dY,$$

where $\overline{Y} = \int_{-\infty}^{\infty} YP(Y)dY$ is the mean position of the "labeled" particles, and $\sigma_Y^2 = \int_{-\infty}^{\infty}(Y-\overline{Y})^2 P(Y)dY$ is their variance.

The results of the corresponding computations (the crosses denote the experiment and the curves refer to computations) are shown in Fig. 5. The results that were derived by model Nos. 1–3 are close to each other and are shown by curve 1. It should be noted that $s_Y < 0$ when the upper wire is heated, and $s_Y > 0$ when the lower wire is heated. As is seen from the experimental data, with increasing x/D the absolute value of the skewness coefficient first increases sharply and then, having reached a maximum, slowly decreases. The skewness of $P(Y)$ [or $T_1(Y)$] decreases even more slowly if the admixture source is positioned in the initial cross section at a distance longer by a factor of two from the wake symmetry plane (curve 2 in Fig. 5, computations by model No. 1).

Curve 3 in Fig. 5 corresponds to the results of calculation of heat diffusion from a line source in a plane momentumless turbulent wake. The distributions of the averaged and fluctuation characteristics of the velocity field were set in agreement with the experimental data of [18]. A comparison of the computation results obtained by model No. 2 with these data can be found in [14]. Fictitious initial conditions were used for the temperature field, since isothermic flow was studied in [18]. The initial distribution of the mean temperature was specified for $x/D = 6$ as a function equal to T_0 outside the region of $0.2 \leqslant y/D \leqslant 0.4$ and to $1.20T_0$ inside this region, and the value of $\langle T'^2\rangle$ was assumed to equal zero everywhere. The term $(\partial/\partial x)(\langle u'^2\rangle - \langle v'^2\rangle) = 2(\partial/\partial x)((\Phi(e/\varepsilon)P)$ was added to the right-hand side of Eq. (2.1) in the computations. Despite the fact that the structure of wakes with zero and nonzero total excess momenta is different, the s_Y behavior is qualitatively the same.

Thus, the data presented indicate that there is no asymptotic state of a plane wake with an asymmetric excess temperature profile and that (sooner or later) the distributions of T_1 will be such as if the entire cylinder were heated (with the same total amount of excess heat).

Not only the mean-temperature distributions but also the profiles of temperature-fluctuation intensity tend to a state that is typical of the flow in the wake behind a fully heated cylinder. This is demonstrated in Fig. 6, where points 1–3 are the measured results for $x/D = 9$, 120, and 200, and the values of $\langle T'^2\rangle^{1/2}$ are normalized to the difference ΔT_0 between the wire temperature T_w and the flow temperature outside the wake: $\Delta T_0 = T_w - T_0 = 460°C$. For small values of x/D, as is seen from the figure, the $\langle T'^2\rangle^{1/2}$ profile shows only one peak, and the profile itself is asymmetric about $y = 0$, whereas, with distance from the cylinder, the distribution of the temperature-fluctuation intensities has two humps, and, even for $x/D = 200$, it takes a form typical of the wake behind plane heated bodies.

The curves in Fig. 6 show the results of computations by model Nos. 1–3 (curves 4 and 5 correspond to model No. 1, where $x/D = 120$ and 200; curves 6 and 7 to model No. 2, and curves 8 and 9 to model No. 3 for the same distances x/D). In spite of the fact that a single-humped experimental profile (points 1) was used as the initial distribution of $\langle T'^2\rangle$, as x/D increases, the solution takes a double-humped asymmetric form, approaching a self-similar solution. The discrepancies observed for $x/D = 200$ are likely to be due to insufficient accuracy of the method of "three overheatings" used for measurements.

With distance from the cylinder, the wake dimensions increase, and the velocity-field and passive-admixture inhomogeneities decay. An idea of the character of these processes is given by the data in Fig.

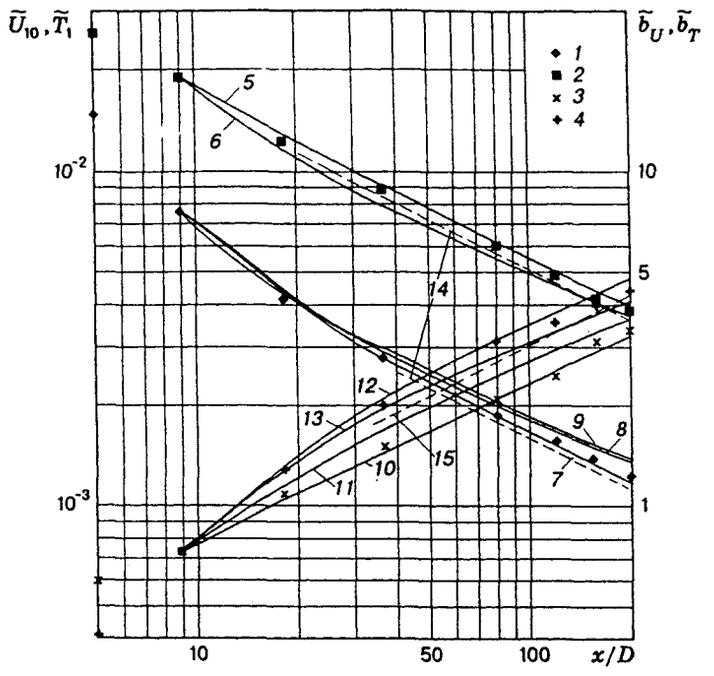

Fig. 7

7, where points 1 refer to $\tilde{U}_{10} = U_{10}/U_0$ (U_{10} is the mean velocity defect at $y = 0$), points 2 refer to $\tilde{T}_1 = T_{1m}/\Delta T_0$, points 3 to $\tilde{b}_U = b_U/D$, and points 4 to $\tilde{b}_T = b_T/D$ [b_U and b_T denote the total width of the $U_1(y)$ or $T_1(y)$ profile at a level of $U_{10}/2$ or $T_{1m}/2$, respectively]. At moderate distances from the heat source, the dimensions of the heated wake region are naturally smaller than the wake width; b_T for $x/D = 5$ is smaller than b_U by a factor of approximately 1.5. However, with increasing x/D, the heat rapidly propagates over the entire cross section of the wake, and $b_T > b_U$ even for $x/D > 10$, which indicates that the momentum and heat turbulent-transfer coefficients are different. Although the distributions of the passive admixture do not reach a self-similar state at the distances from the cylinder studied in the experiments, for large x/D, both b_U and b_T are proportional to $x^{1/2}$ (curve 15 in Fig. 7) and, hence, their ratio is nearly constant and is equal to 0.76. Note that close values of b_U/b_T were also obtained in a plane heated jet (0.74 in [19]) and in the wake behind a circular cylinder (0.76 in [20] and 0.80 in [21]). The reduction in the maximum excess temperature for large x/D is practically proportional to $x^{-1/2}$ (curve 14), which agrees with the decay laws derived in [2] for self-similar flows in a plane wake.

The numerical results are shown by curves 5–13 in Fig. 7. Curves 5 and 6 describe the variation of the axial value of velocity defect versus the distance from the body, curve 5 is obtained using model No. 1, curve 6 using model Nos. 2 and 3. Curves 7–9 show the decay of the maximum value of the temperature defect $\widetilde{T_1}$ and correspond to the calculations by model Nos. 1–3. The variation of the calculated values of b_U and b_T is represented by curves 10, 11 and 12, 13 (curves 10 and 12 are plotted using model No. 1, and curves 11 and 13 using model No. 2). The values of b_T calculated by model Nos. 2 and 3 practically coincide (curve 13).

A comparison of the computed and experimental data (Figs. 2–7) and also the numerical results for plane wakes with zero and nonzero excess momenta [12] and for axisymmetric wakes [11] allow one to draw the conclusion that the algebraic models of Reynolds stresses [10] and heat fluxes [13] are universal enough, since all computations were performed with the same set of empirical constants.

The data obtained in experiments and mathematical simulation make it possible to picture the passive admixture transport in a plane wake as follows. In the immediate vicinity of a source, the admixture is localized in a thin sheet, which is deformed, with distance from the source, under the action of larger-scale turbulent vortices and is also smeared because of molecular diffusion. Since the dimensions of large vortices

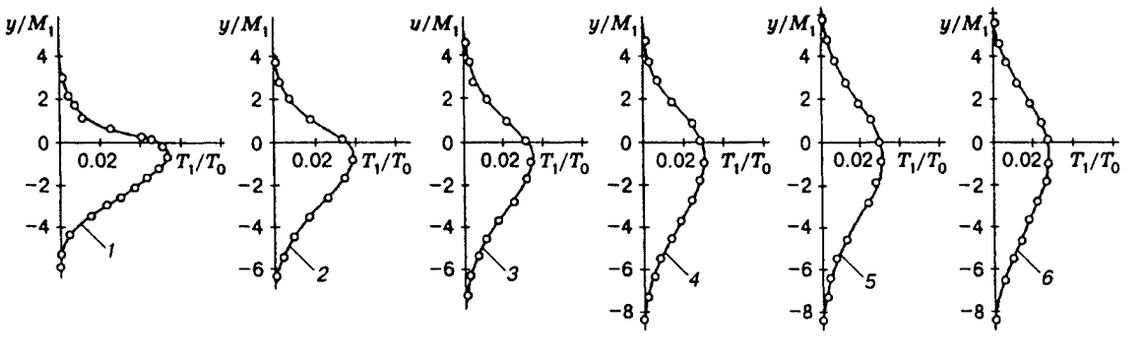

Fig. 8

is comparable with the transverse dimensions of the wake, the admixture is quickly spread over its entire width, remaining concentrated in strongly deformed but comparatively narrow regions and causing a strong intermittency of instantaneous concentration of the admixture. The admixture is predominantly transferred to the region of large-scale vortices so that the distributions of the mean admixture concentration and admixture fluctuation intensity attain, with time, the same type of symmetry as the scale distributions of vortices.

The predominant admixture transfer by large-scale vortices in flows with a weakly varying mean velocity (and such are far wakes) is also evidenced by the results of special experiments on passive-admixture diffusion in shearless inhomogeneous turbulence behind a combined grid. An experimental setup (without an admixture source), a coordinate system, the nomenclature used, and the velocity-field turbulent characteristics can be found in [22]. A line source of admixture (heat) was located in the plane $y = 0$ along the z axis and $5M_1$ apart the grid. With the grid ratio $M_2/M_1 = 5$, the compound grid generates turbulence with $u_-^2/u_+^2 \approx 10$ and $L_-/L_+ \approx 1.8$, where L_- and L_+ are the integral turbulence scales in homogeneous regions behind the coarse and fine parts of the compound grid, respectively.

The character of heat propagation from a line source in inhomogeneous shearless turbulence is illustrated in Fig. 8, which shows the mean-excess-temperature profiles. Curve numbers 1–6 indicate the corresponding distances from the grid $x/M_1 = 40$, 80, 120, 160, 200, and 240, and the curves were plotted using experimental data. One can see that when there are no mean-velocity gradients, the passive-admixture-concentration distributions are formed in such a way that a major portion of the admixture appears in the region of large-scale turbulent flows.

This work was supported by the Russian Foundation for Fundamental Research (Grant 95-01-00910).

REFERENCES

1. J. O. Hinze, *Turbulence. An Introduction to Its Mechanism and Theory*, McGraw–Hill, New York (1959).
2. A. S. Monin and A. M. Yaglom, *Statistical Hydromechanics* [in Russian], Gidrometeoizdat, Saint Petersburg (1992), Part 1.
3. B. B. Ilyushin and A. F. Kurbatskii, "Application of second-order momentum equations to the problem of diffusion of admixture from a line source," *Sib. Fiz.-Tekh. Zh.*, No. 5, 25–35 (1993).
4. U. Karnik and S. Tavoularis, "Measurement of heat diffusion from a continuous line source in a uniformly sheared turbulent flow," *J. Fluid Mech.*, **202**, 233–261 (1989).
5. M. K. Chung and N. H. Kyong, "Measurement of turbulent dispersion behind a fine cylindrical heat source in a weakly sheared flow," *J. Fluid Mech.*, **205**, 171–193 (1989).
6. H. Stapountzis and R. E. Britter, "Turbulent diffusion behind a heated line source in a nearly homogeneous turbulent shear flow," in: *Turbulent Shear Flows*, Springer, Berlin (1989), Vol. 6, pp. 97–108.

7. S. Veeravalli and Z. Warhaft, "Thermal dispersion from a line source in the shearless turbulence mixing layer," *J. Fluid Mech.*, **216**, 35–70 (1990).
8. D. J. Shlien and S. Corrsin, "Dispersion measurements in a turbulent boundary layer," *Int. J. Heat Mass Transfer*, **19**, No. 3, 285–295 (1976).
9. P. Paranthoen and M. Trinite, "Etude de la diffusion de la chaleur en aval d'une source lineaire placee dans une couche limite turbulente," *Int. J. Heat Mass Transfer*, **24**, No. 7, 1105–1113 (1981).
10. W. Rodi, *Turbulence Models and their Application in Hydraulics*, Univ. of Karlsruhe, Karlsruhe (1980).
11. N. N. Fedorova and G. G. Chernykh, "On numerical simulation of a momentumless wake behind a sphere," in: *Modeling in Mechanics* [in Russian], Inst. of Theor. and Appl. Mech., Sib. Div., Russian Acad. of Sci., **6(23)**, No. 1 (1992).
12. G. G. Chernykh, A. G. Demenkov, and N. N. Fedorova, "Numerical models of plane and axisymmetric turbulent wakes in homogeneous fluid," in: Int. Conf. on the Methods of Aerophysical Research, Aug. 22–26, 1994, Novosibirsk (1994), Part 2, pp. 76–81.
13. M. M. Gibson and B. E. Launder, "On the calculation of horizontal turbulent free shear flows under gravitational influence," *Trans. ASME*, **C98**, No. 1, 81–87 (1976).
14. A. G. Demenkov and G. G. Chernykh, "On numerical simulation of viscous incompressible jet flows," in: *Computational Technologies* [in Russian], Inst. of Computational Technol., Sib. Div., Russian Acad. of Sci., **4**, No. 12 (1995).
15. P. Freymuth and M. S. Uberoi, "Structure of temperature fluctuations in the turbulent wake behind a heated cylinder," *Phys. Fluids*, **14**, No. 12, 2574–2580 (1971).
16. Yu. M. Lytkin, "Turbulent wake behind a cylinder of noncircular cross section," in: Dynamics of Continuous Media [in Russian], Institute of Hydrodynamics, Novosibirsk, **5** (1970).
17. S. Corrsin, "Extended applications of the hot-wire anemometer," NASA Technical Note No. 1864 (1949).
18. Yu. M. Dmitrenko, I. I. Kovalev, N. N. Luchko, and P. Ya. Cherepanov, "Study of a plane turbulent wake with zero excess momentum," *Inzh.-Fiz. Zh.*, **52**, No. 5, 743–751 (1987).
19. A. S. Ginevskii, *Theory of Turbulent Jets and Wakes* [in Russian], Mashinostroyenie, Moscow (1969).
20. A. A. Townsend, *The Structure of Turbulent Shear Flow*, Cambridge Univ. Press (1956).
21. M. S. Uberoi and P. Freymuth, "Spectra of turbulence in wakes behind circular cylinders," *Phys. Fluids*, **12**, No. 7, 1359–1363 (1969).
22. N. V. Aleksenko, V. I. Bukreev, and V. A. Kostomakha, "Shearless interaction of two isotropic turbulent fields," *Zh. Prikl. Mekh. Tekh. Fiz.*, No. 1, 57–62 (1985).